

Computation of Cross-Polarisation Due to Rain over Durban, South Africa

¹Oluwumi Adetan, ²Thomas.J. Afullo

Abstract—The aim of this paper is to compute the cross polarisation caused by rain (XPD) at frequency band 10-35 GHz over Durban (29°52'S, 30° 58'E), a city along the eastern coast of South Africa. Two elevation angles of 23° and 55° are assumed for wave propagation along the coastal region. The globally accepted lognormal drop size distribution model for tropical region has been used to compute the raindrop sizes assumed to be spherical at 20°C. The power law relationship between attenuation and rain rate based on the measured complimentary cumulative distribution of rain rates in Durban is used to estimate the total attenuation. The ITU-R procedure in recommendation 618-9 (ITU-R, 2007) is employed in the estimation of the cross polarisation discrimination due to rain on earth-satellite path. From our results, a linear difference of about 9dB between 0.1% and 0.01% of time is observed at all frequencies over the elevation angles. The XPD observed at 0.1% of time is higher than that of 0.01% at the same elevation angle and frequency. A lower value of XPD results in higher cross-talk or high interference between the two orthogonal channels at the satellite receiver station. The variation of the estimated values of XPD with co-polar attenuation (CPA), frequencies and rain rates at these elevation angles is also examined. The circular polarisation for earth-satellite propagation paths is assumed for the purpose of analysis.

Keywords— Depolarisation, Cross polarisation discrimination (XPD); Copolar attenuation (CPA); Cross-talk.

1 INTRODUCTION

The orientation of the lines of the electric flux in an electromagnetic (EM) field is generally referred to as wave polarisation. The use of orthogonal polarisations allows two independent information channels using the same frequency band to transmit signals over a single link. This method is useful in satellite communication systems to effectively increase the available spectrum. However, some degrees of interference between these channels are inevitable due to depolarizing effects caused by scattering and absorption of the hydrometeor (rain, ice, etc.), along the propagation path. This depolarisation is due to the non-spherical symmetry of the raindrops (the top and bottom are flattened), along with their tendency to have a preferred orientation. Depolarisation results in cross talk between two orthogonal polarized channels, transmitted on the same path and frequency band [1]-[7]. As a result of this, radiowaves propagating through them suffers differential attenuation and phase shift. This also may constitute a problem in communication systems using polarisation orthogonality to maintain isolation between channels. Differential attenuation and phase below 18 GHz increases with frequency for a given rain event, they however decrease for a given fade depth [1]. This is partly because less deformed smaller drops make a greater relative

contribution to the total attenuation as frequency is increased.

Polarisation can be linear or circular (elliptical). The most general case of polarisation is the elliptical or circular polarisation. The electric field vector $\mathbf{E}(t)$, as expressed by [2] in equation (2) composed of two sinusoidal components, having different amplitudes $|E_x|$ and $|E_y|$ and a phase difference $\arg\left(\frac{E_y}{E_x}\right)$:

$$\mathbf{E}(t) = R_e \mathbf{E} e^{j\omega t} = R_e [(u_x E_x + u_y E_y) e^{j\omega t}] \quad (1)$$

$$= u_x |E_x| \cos(\omega t) + u_y |E_y| \cos(\omega t + \phi) \quad (2)$$

where u_x and u_y are the units vectors in the x- and y- directions respectively; ω is the angular frequency and t is the time. The phase is taken relative to the phase of E_x . As observed in (1), the polarisation may be frequency dependent and time varying as the hydrometeor change. Oftentimes, EM waves transmitted along the principal planes will arrive unchanged (magnitude) but, experience differential attenuation and phase shifts. Consequently, any transmitted polarisation that is not one of the link's principal planes will be cross polarized on reception [1-2]. It is important to mention that the relative contribution of differential attenuation and phase shift is different at different frequencies. Differential phase shift appears to be the dominant factor in rain induced depolarisation at frequencies below 10 GHz and differential attenuation becomes increasingly significant at higher frequencies. Linearly polarized waves have an infinite axial ratio (the ratio of the maximum to the minimum magnitude of the electric field vector) while circularly polarized waves have an axial ratio that lies between +1 and -1, corresponding to

¹Oluwumi Adetan is currently pursuing his doctoral degree program in electronic engineering in University of KwaZulu-Natal South Africa. His research interest is to study the effects of rain on microwave and communication systems. E-mail: oadetan@gmail.com.

²Thomas J. Afullo is a Professor in the School of Engineering, University of KwaZulu-Natal, South Africa. His research interest includes communication systems, electromagnetic theory, microwave and R F communications. E-mail: afullot@ukzn.ac.za

either left-hand circular polarisation (LHCP) or right-hand circular polarisation (RHCP) [2].

A reliable estimate of the depolarizing properties of tropical rainfall for terrestrial and earth space links therefore requires among other parameters; the investigation of the differential attenuation, differential phase shift, cross polarisation discrimination (XPD) in the orthogonal channels and the co-polar attenuation (CPA). The aim of this paper is to estimate the cross polarisation of millimeter waves in the Ku and Ka band frequencies caused by rainfall over Durban (29°52'S, 30° 58'E) at two elevation angles of 23° and 55° at frequency range 10-35 GHz. The elevation angles 23° and 55° are for links above the Indian Ocean Region (IOR) and over the Atlantic Ocean Region (AOR) respectively. The ITU-R P.618-9 [8]; recommendation for propagation data and prediction methods required for the design of Earth-space telecommunications systems is adopted for the purpose of computation. An attempt is made to determine the variation of the XPD with co-polar attenuation (CPA), rainfall rate and frequency. The raindrop sizes are assumed spherical at 20°C and the circular polarisation for Earth-satellite propagation paths is also assumed for the purpose of computation.

2 OVERVIEW OF RELATED WORKS AND EXPERIMENTAL SET UP

2.1 Related Work

A good number of researchers have determined the propagation effects of cross polarisation caused by rain. Experimental results have shown the existence of a relationship between attenuation and depolarisation especially when rain depolarisation is dominant. This has been extensively discussed by *Nowland et al.*[9], *Dissanayake et al.*[10] and *Chu* [11]. In their separate studies, *Ajewole* [4] and *Oguchi* [5] showed that rain induced cross polarisation of radio waves has its roots in the differential attenuation and differential phase shift produced between the two polarisation states and in the slight tilt of the axis of symmetry (canting angle) of the raindrop away from the vertical due to wind effects. By assuming a constant canting angle of raindrops along a propagation path, *Oguchi* and *Hosoya* [12] estimated the cross polarisation due to different rainfall rates. Similarly, *Ajewole et al.* [13] computed XPD due to rain for four tropical types of rain by adopting the method earlier proposed by *Oguchi* [14]. The effects of varying the canting angles of the raindrops was also investigated by *Ajewole et al.* [15] using different types of rain and raindrop sizes on cross polarisation discrimination and established that XPD improves by about 4-7 dB over those models having equal orientation. Recently, the dependence of XPD on co-polar attenuation, frequency and rainfall was estimated by *Ojo* [16] over some stations in Nigeria at various elevation angles and frequencies.

In this work, the computation of XPD at frequency range 10-35 GHz and at elevation angles of 23° and 55° is carried

out over the eastern coast of South Africa assuming a spherical raindrop sizes at 20°C. The variation of the estimated values of XPD with other parameters such as co-polar attenuation, rain rate and frequency is also discussed.

2.2 Experimental Set Up

Durban (29°52'S, 30° 58'E) is a coastal city located along the eastern coast of South Africa. The city is characterized by four different seasons per annum. It is often referred to as a humid subtropical region due to its high rainfall intensity which often occurs during the summer months [17-19].

In this report, the rainfall rate data measured over a period of one year (January - December, 2009) using a Joss-Waldvogel (JW) RD-80 disdrometer measuring system has been utilized to estimate the cross polarisation caused by rain over Durban. The equipment is installed at the roof top of the School of Electrical, Electronic and Computer Engineering building, University of KwaZulu Natal, (Howard College), South Africa. The minimum and

TABLE 1
 RAIN RATE DISTRIBUTION AT VARIOUS PERCENTAGES OF EXCEEDENCE IN DURBAN

maximum rainfall rate values are 0.003mm/h and 117.15mm/h respectively. The disdrometer converts the momentum of each falling drop impacting on the sensor's surface into an electric pulse of commensurate voltage. The detectable diameter range is divided into 20 intervals [20].

Percentage of time Rainfall rate is exceeded (%)	Rainfall Rate (mm/h)
2	6.62
1	10.53
0.5	16.21
0.3	20.96
0.2	24.26
0.1	32.33
0.05	47.57
0.03	51.67
0.02	57.35
0.01	66.25

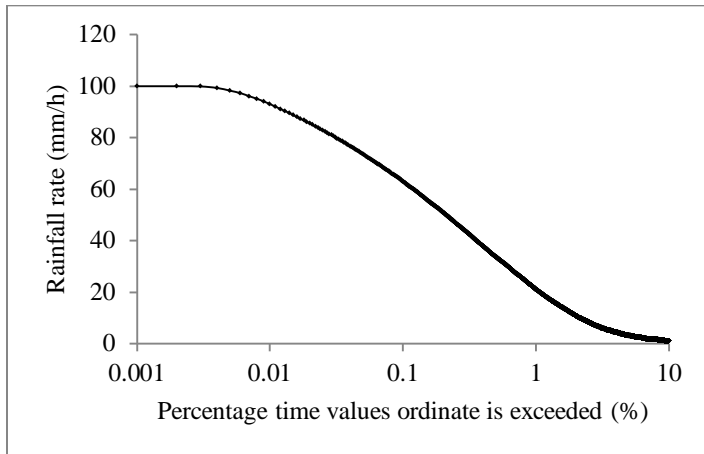


Fig.1. Rainfall rate complementary cumulative distribution function (CDDF) for Durban (Jan -Dec. 2009).

The sampling time, T of the disdrometer is 60s with the sampling area, A of $50cm^2$ ($0.005 m^2$). Rainfall samples with overall sum of drops less than 10 were discarded to compensate for the dead-time errors. The instrument is located at an altitude of $139.7m$ above sea level. Although there is generally high wind variability in Durban, the location site is free of disturbances due to unwanted noise and shielded from abnormal winds. Fig.1 and Table 1 show the complementary cumulative distribution function (CDDF) of the rainfall rate for the one year data in Durban and the specific relationship between the percentages of time the rain rate is exceeded. Rainfall rate values of $32.33 mm/h$, $66.25mm/h$ and $101.56mm/h$ were estimated at 0.1%, 0.01 % and 0.001 % of time exceeded respectively.

3 COMPUTATIONAL PROCEDURES

The ratio (in dB) of the power in the copolarised wave to the power in the crosspolarised wave that was transmitted in the same state is termed the cross polarisation discrimination due to rain ($XPDR_{rain}$). In other words, it is the appearance in the course of propagation of a radio wave through the atmosphere, of a polarisation component which is orthogonal to the desired polarisation.

Mathematically, it can be expressed by [2]-[5] as:

$$XPDR_{rain} = 20\log_{10} \left| \frac{E_{xx}}{E_{xy}} \right| \quad (dB) \quad (3)$$

where E_{xx} and E_{xy} are the co-polarized and cross polarized waves transmitted in the same polarisation states respectively. The ITU-R step-by step methods to compute the $XPDR_{rain}$ statistics are stated as follows:

Step 1: Calculate the frequency-dependent term:

$$C_f = 30 \log f \text{ for } 8 \leq f \leq 35 \text{ GHz} \quad (4)$$

where f is the frequency in GHz .

Step 2: Calculate the rain attenuation dependent term:

$$C_A = V(f) \log A_p \quad (5)$$

where A_p is the estimated rainfall attenuation (in dB) exceeded for the required percentages of time. This may also be computed from [7].

$$V(f) = 12.8 * f^{0.19} \quad \text{for } 8 \leq f \leq 20 \text{ GHz}$$

$$V(f) = 22.6 \quad \text{for } 20 < f \leq 35 \text{ GHz}$$

Step 3: Calculate the polarisation improvement factor:

$$C_\tau = -10 \log[1 - 0.484(1 + \cos 4\tau)] \quad (6)$$

where $C_\tau = 0$ for $\tau = 45^\circ$ and reaches the maximum value of 15 dB for $\tau = 0^\circ$ or 90° .

Step 4: Calculate the elevation angle dependent term:

$$C_\theta = -40 \log(\cos \theta) \quad \text{for } \theta \leq 60^\circ \quad (7)$$

Step 5: Calculate the canting angle dependent term:

$$C_\sigma = 0.0052\sigma^2 \quad (8)$$

where σ is the effective standard deviation of the raindrop canting angle distribution (in degrees). It takes the value 0° , 5° , 10° and 15° for 1%, 0.1%, 0.01% and 0.001% of the time respectively. In this work, the value of 10° is used.

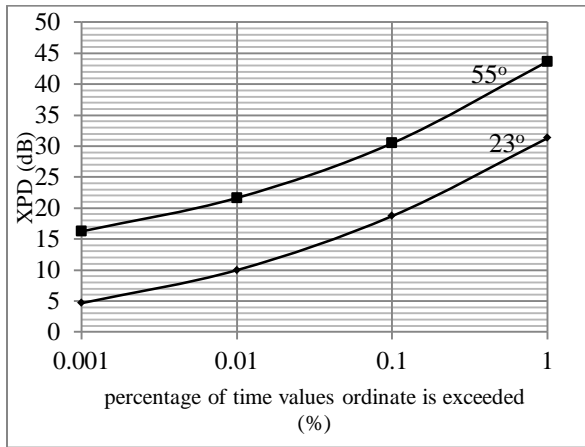
Step 6: Calculate rain $XPDR$ not exceeded for $p\%$ of the time:

$$XPDR_{rain} = C_f - C_A + C_\tau + C_\theta + C_\sigma \quad (dB) \quad (9)$$

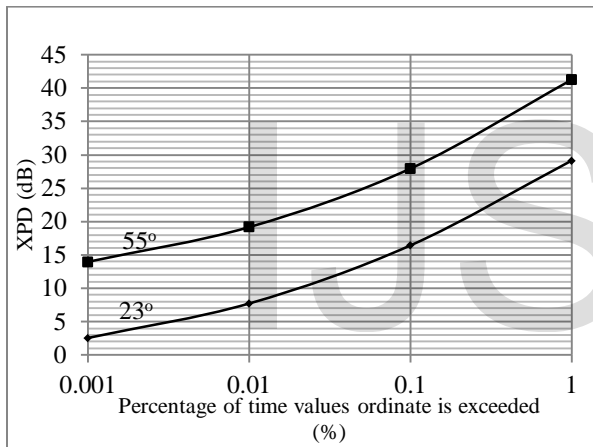
4 RESULTS AND DISCUSSIONS

The variation of $XPDR$ at various elevation angles and frequencies 12, 15, 20 and 35 GHz are shown in Fig. 2. In general and at all frequencies, $XPDR$ decreases as frequency increases for all the elevation angles. As the elevation angle increases for a given frequency, the $XPDR$ increases. A larger value of $XPDR$ is observed as the percentage of time also increases. A difference of about 8-9 dB is observed between 0.1 % and 0.01% of time while a difference of about 5-6 dB is noticed between 0.01 % and 0.001% of time. A low value of $XPDR$ implies an increased interference (cross-talk) at the receiver station of the satellite. The following sub-sections further explain the variation of $XPDR$ with co-polar

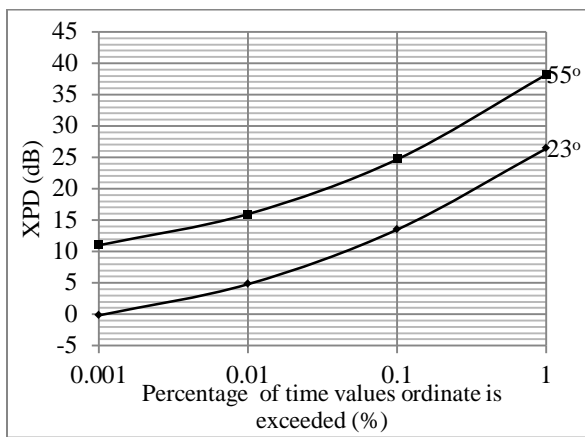
attenuation, rainfall rate and operating frequencies for different elevation angles.



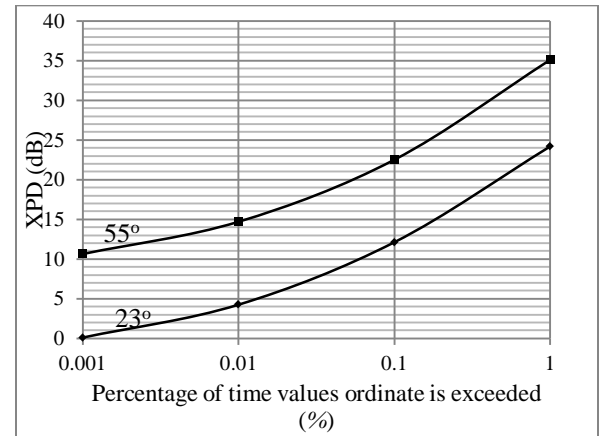
(a) 12 GHz



(b) 15 GHz



(c) 20GHz

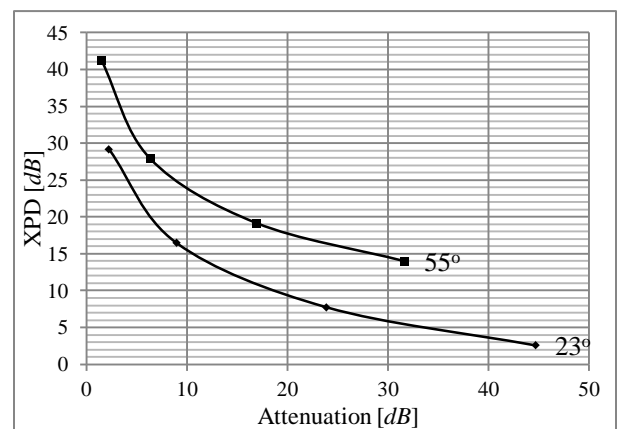


(d) 35GHz

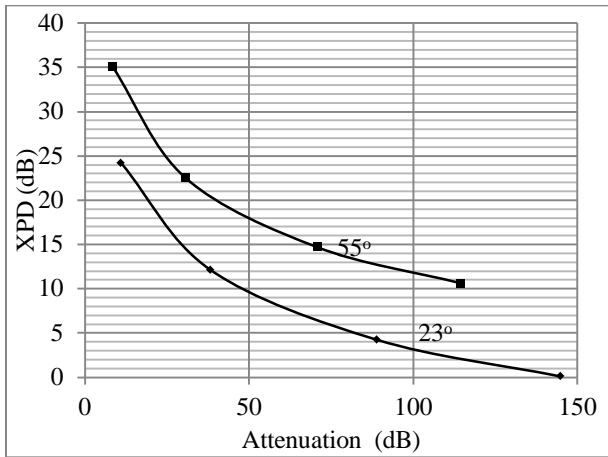
Fig.2. Cross polarisation discrimination (XPD) over different elevation angles at $f = 10\text{-}35\text{ GHz}$ in Durban ($R_{0.01} = 66.25\text{ mm/h}$).

4.1 XPD-CPA Relations in Durban

Fig.3 shows the variation of the XPD and the rain attenuation exceeded for the required period of time, often called the co-polar attenuation (CPA) over the elevation angles at (a) $f = 15\text{ GHz}$ and (b) 35 GHz . It can be observed that the CPA increases with decreasing angle of elevation. The cross polarisation discrimination degrades with increasing CPA. This shows an agreement with *Ajewole et al.* [13] and confirms the inverse relation between the CPA and XPD. This implies that signal degradation as a result of XPD is enhanced more by CPA for a given fade than due to XPD as the frequency decreases.



(a)



(b)

Fig. 3. XPD versus Co-polar attenuation

4.2 Variation of XPD with Frequency

It is important to mention that the relative contribution of differential attenuation and phase shift is different at different frequencies. Differential phase shift appears to be the dominant factor in rain induced depolarisation at frequencies below 10 GHz and differential attenuation becomes increasingly significant at higher frequencies. The dependence of XPD on frequency at the elevation angles for different rain event is shown in Table 2. In general and for all the elevation angles, XPD decreases as the frequency of operation increases. However, at higher frequency above 30 GHz, a sharp change in XPD values is observed. This may be due to the presence of ice crystals in the upper layer of rainclouds producing a greater contribution to depolarisation. Similarly, less deformed smaller drops make a greater relative contribution to the total attenuation as frequency is increased. The contributions of the differential attenuation and phase shift to cross polarisation at varying frequencies and the complex dielectric property of water which depends on frequency are also probable factors that may be responsible for the sudden change in the XPD as the frequency increases. The differential propagation reduces with frequency for a given fade depth.

TABLE 2
 VARIATION OF XPD WITH FREQUENCY FOR
 DIFFERENT ELEVATION ANGLES
 (a) $R_{0.01}$, (b) $R_{0.1}$.

f (GHz)	12	15	20	30	35
23°	31.297	29.139	26.407	24.497	24.202
	18.714	16.431	13.497	12.214	12.117
	9.978	7.726	4.801	4.142	4.242
	4.648	2.562	-0.170	-0.207	0.091
55°	43.667	41.259	38.188	35.609	35.119
	30.469	27.948	24.688	22.795	22.518
	21.636	19.176	15.969	14.757	14.695
	16.234	13.975	11.007	10.474	10.627

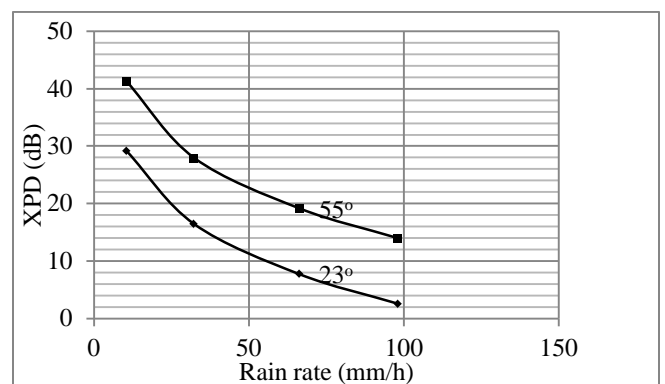
(a)

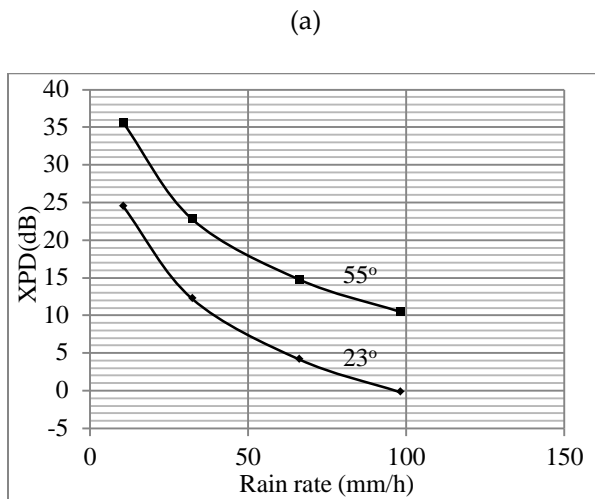
f (GHz)	12	15	20	30	35
23°	36.249	34.169	31.567	29.319	28.869
	23.240	21.028	18.214	16.622	16.383
	14.079	11.892	9.075	8.136	8.108
	8.324	6.296	3.661	3.373	3.556
55°	48.806	46.502	43.610	40.749	40.121
	35.168	32.739	29.645	27.494	27.092
	25.892	23.518	20.461	19.015	18.839
	20.049	17.867	15.033	14.291	14.342

(b)

4.3 XPD versus Rainfall Rate

The variation of XPD with rain rate at (a) $f = 15$ GHz and (b) $f = 30$ GHz is given in Fig 4 and Table 3 at the two elevation angles. An inverse relation is also observed between the XPD and rainfall rate at all angles of elevation. As the rainfall rate increases, XPD decreases. Table III shows the XPD-rain rate relation at different elevation angles operating at $f = 12$ and 30GHz. At a given rain rate, the cross polarisation discrimination increases with increase in elevation angles. The cross polarisation becomes poorer as the rain rate and frequency are raised. This results in poor interference level in the orthogonal channels.





(b)
 Fig. 4. XPD versus rainfall rate at (a) $f = 15\text{GHz}$ (b) $f = 30\text{GHz}$

TABLE 3
 COMPUTED XPD VALUES AND RAINFALL RATES AT OPERATING FREQUENCIES of 12 and 30 GHz.

12 GHz					
$R_{0.01}$ (mm/h)		10.53	32.33	66.25	98.16
Elevation angle	23°	31.297	18.714	9.978	4.648
	55°	43.667	30.469	21.636	16.234
30 GHz					
Elevation angle	23°	24.497	12.214	4.142	-0.207
	55°	35.609	22.795	14.757	10.474

5 CONCLUSION

The reliability of a transmission link is mostly determined from the quantities measured at one time or the other on the link. The computation of cross polarisation discrimination and its relationship to co-polar attenuation and other quantities along the Earth-space propagation paths at elevation angles of 23° and 55° and frequency band 10-35GHz has been carried out in this work. Our results show that cross polarisation discrimination degrades with increasing co-polar attenuation and decreases sharply as the elevation angle decreases due to the larger attenuation as a result of longer distance the signal travels at low

elevation angles. The results obtained in this work will greatly be useful in the design of terrestrial and Earth-to-satellite link in southern Africa. However, due to inadequate of experimental data, it will be of interest to further investigate and validate this work in the nearest future and to estimate same for other regions across South Africa.

ACKNOWLEDGEMENT

Fruitful discussions with Professor Moses O. Ajewole and Dr. Joseph S. Ojo of the Center for Research and Developments (CERAD), Akure, Nigeria are highly appreciated.

REFERENCES

- [1] L. Barclay, (Ed.), "Propagation of radiowaves," The Institution of Electrical Engineers, 2nd edition, 2003.
- [2] G. Brussaard and P.A. Watson, "Atmospheric modelling and millilitre wave propagation," Chapman and Hall, London SE1 8HN, 1st edition, United Kingdom, 1995.
- [3] G.O. Ajayi, "Some tropical rainfall and their effect on microwave propagation," *International journal of satellite communication*, Vol. 8, pp.163-172, 1990
- [4] M.O. Ajewole, and B.O. Afolayan, "Rain induced depolarisation scaling parameters for linearly polarized SHF waves communication on earth-space paths in Nigeria," *Global journal of pure and applied sciences*, Vol. 14, No.2, pp. 235-240, 2008.
- [5] T. Oguchi., "Electromagnetic wave propagation and scattering in rain and other hydrometeor," *Proceedings of IEEE*, Vol. 71, No.9, pp. 1029-1078, 1983.
- [6] M.O. Ajewole, "Scattering and attenuation of centimeters and millimeters radio signals by tropical rainfall," Ph.D. Thesis, Federal University of Technology, Akure, Nigeria, 1997.
- [7] M.M.J.L. Van de Kamp, "Depolarisation due to rain: the XPD-CPA relation," *Int. J. Satell. Commun.* 19; 285-301, DOI: 10.1002/sat.672, 2001.
- [8] ITU-R P.618-9 Propagation data and prediction methods required for the design of Earth-space telecommunications systems, Recommendation P, ITU-R Ser., *Inter. Telecomm Union*, Geneva, Switzerland, 2007.
- [9] W.L. Nowland, R.L. Olsen and I.P. Sharkofsky, "Theoretical relationship between rain depolarisation and attenuation," *Electronic letters*, No. 13, pp. 676-678, 1977.
- [10] A.W. Dissanayake, D.P. Haworth and P.A. Watson, "Analytical models for cross polarisation on Earth-space radio paths for frequency range 9-30GHz," *Antenna Telecomm.*, Vol.35 No 16, pp. 398-404, 1980.
- [11] T.S.A. Chu, "A Semi-empirical formula for microwave depolarisation versus raindrop attenuation on Earth-space paths," *IEEE Trans. Commun.*, COM-30, No. 12, 2550, 1982.
- [12] T. Oguchi, and Y Hosoya, "Scattering properties of oblate raindrops and cross-polarisation of radio wave due to rain, Part II: Calculation at microwave and millimeter wave regions," *J. Radio Res Lab*, Jpn 21:191-259, 1974.

- [13] M.O. Ajewole, L.B. Kolawole and G.O. Ajayi, "Theoretical study of the effect of different types of tropical rainfall on microwave and millimeter-wave propagation," *Radio Sci.* 34(5):1103-1124, 1999.
- [14] T. Oguchi, "Scattering properties of oblate raindrops and cross-polarisation of radio waves due to rain: Calculations at 19.3 and 34.8GHz," *J. Radio Res Lab, Jpn* 20(102): 79-118, 1973.
- [15] M.O. Ajewole, L.B. Kolawole and G.O. Ajayi, "Cross polarisation of line-of-sight links in a tropical location: effects of the variation in canting angle and drop size distribution," *IEEE Trans on Ant. Propag.* 47 (8): pp.1-6, 1999.
- [16] J.S. Ojo, "Estimation of cross-polarisation due to rain over some stations in Nigeria," *Ann. Telecomm* DOI 10.1007/s12243-011-0269-4, 67:241-245, 2012.
- [17] <http://www.biztradeshows.com/southafrica/durban/durban.html>
- [18] M.O. Fashuyi, P.A. Owolawi and T.O. Afullo, "Rainfall rate modeling for LOS radio systems in South Africa," *Trans. of South African Institute of Electrical Engineers (SAIEE)*, Vol. 97, pp.74-81, 2006
- [19] <http://www.ceroi.net/reports/durban/drivers/Climate/index.htm>
- [20] M.J. Bartholomew, "Disdrometer and tipping bucket rain gauge handbook," DOE/SC-ARM/TR-079, ARM Climate Research Facility, December 2009.

IJSER